A Comparison of the Performance of Modular Standalone Do-It-Yourself Ion Mobility Spectrometry Systems

Cameron N. Naylor¹, Elvin R. Cabrera¹, Brian H. Clowers^{1*}

Abstract:

As the spectrum of ion mobility spectrometry (IMS) applications expands and more experimental configurations are developed, identifying the correct platform for an experimental campaign becomes more challenging for researchers. Additionally, metrics that compare performance (R_{p.} for example) often have nuanced differences in definition between platforms that render direct comparisons difficult. Here we present a comparison of three do-it-yourself (DIY) drift tubes that are relatively low cost and easy to construct, where the performance of each is evaluated based on three different metrics: resolving power, the ideality of resolving powers, and accuracy/precision of K₀ values. The standard PCBIMS design developed by Reinecke and Clowers (Reinecke, T.: Clowers, B. H., HardwareX 2018, 4) provided the highest resolving power (> 90) and the highest ideality of resolving power ratios (>90% at best) of the three systems. However, the flexible tube (FlexIMS) construction as described by Smith et al. (Smith, B. L. et al. Anal. Chem. 2020, 92 (13), 9104-9112) exhibited the highest degree of precision of K₀ values (relative standard deviation < 0.42 %). Depending on the application, the drift tube variants presented and evaluated here offer a low-cost alternative to commercial drift-tube systems with levels of performance that approach theoretical maxima.

Keywords: ion mobility spectrometry, open-source, experimental design, resolving power

¹ Department of Chemistry, Washington State University, Pullman, WA 99164, United States *Corresponding Author: Brian H. Clowers (brian.clowers@wsu.edu)

Introduction

Given the insights afforded by coupling ion mobility spectrometry (IMS) with mass spectrometry (MS), there is a persistent drive to optimize and enhance gas-phase ion separations to capture information that extends beyond the information provided by measuring m/z alone. Specifically, value exists in evaluating the relative size of gas-phase ions and whether they adopt expanded or compact conformation in the gas phase. 1-3 In fact, over the past 25 years, the number of IMS papers in the literature has increased by over an order of magnitude including multiple novel instrumental configurations that exploit gas-phase ion mobility that are now commercially available.^{4,5} While the trapped ion mobility spectrometer (TIMS),^{6,7} traveling wave ion mobility spectrometer (TWIMS),^{8,9} and structures for lossless ion manipulations (SLIM)¹⁰ are all relatively new configurations, each with their own advantages and disadvantages, the most widely used IMS platform remains the drift tube ion mobility spectrometer (DTIMS).⁵ The majority of these DTIMS platforms are used for security purposes, such as screening for explosives or narcotics at international borders and public transit hubs. 11,12 While commercial research-grade DTIMS systems are available, these systems, by definition, lack flexibility and require considerable capital investment. 13-16

To meet the instrumental versatility often required in a research environment, there have been multiple attempts to design lower-cost DIY IMS instruments. Such efforts include the recent flexible drift tube IMS design by Smith et al., where an IMS is produced by rolling a flexible printed circuit board (PCB) with electrode strips into a tube. ¹⁷ An additional series of lower-cost drift tube designs has been presented by the Zimmermann group, that include printed circuit boards with optimized pitch and width of the electrodes to provide the best performance and most uniform electric field. ¹⁸ More recently, Ahrens et al. presented a miniaturized drift tube of stainless steel straps and a composite stacked PCB design with alternating metal sheets and insulative layers, ^{19,20} and Bohnhorst et al. updated the PCB design to allow for a moving electric field to be applied throughout the tube. ²¹ Other notable designs include a 3-D printed drift tube described separately by several groups, including Hauck et al. and Hollerbach et al., ^{22,23} and the stacked PCB

design from Reinecke and Clowers.²⁴ While each of these designs provides its own approach to a low-cost alternative commercial instrumentation, an important question to consider is what compromises must be made when relying upon open-source instrumental IMS designs?

IMS performance is typically classified in one of two terms: resolving power and/or resolution.^{25,26} Mathematically, resolution (R) compares the relative separation of two peaks and is used extensively in chromatography.²⁶ Resolving power (R_p), on the other hand, is a single-peak metric and is the ratio of centroid of the arrival time distribution to its absolute peak width at half height more commonly employed to characterize mass spectrometers. Under ideal operating conditions, Rp is a reasonable substitution for resolution, however, is ultimately flawed as the ratio of the smallest to lowest mobility that can be probed using a drift tube is constrained due to practical limitations and a non-linear relationship between drift time and thermal diffusion as defined by Brownian motion.^{25,27} In the early 2000's the Hill group standardized resolution (i.e. the separation of 2 peaks) by introducing separation factors (a ratio of peak mobilities compared to each other),²⁸ but outside of the Hill group, this metric has seen little use.^{28–30} Despite its limitations, R_D remains the most wide-spread metric of IMS performance with respect to separation capacity. Ignoring the practical limitations, the theoretical resolving power depends on the width of the initial gate pulse width and thermal diffusion. Combined, these two factors comprise the full width half maximum of an arrival time distribution in a DTIMS. When environmental factors are completely controlled (e.g. temperature, gas homogeneity, and ion desolvation) and the electric field applied is homogeneous, the observed resolving power in an instrument is a direct measure of ion packet fidelity as it traverses the drift cell. 13,25,27,31 Often physical limitations resulting in a decrease in resolving power include the electric field heterogeneity, ion gate depletion, and Coulombic repulsion to name but a few.^{25,27} Caution is warranted, however, when invoking the spectre of Coulombic repulsion as the conditions for this behavior requires considerable levels of ion current (i.e. $> 5.26 \times 10^7$ C/cm³ at atmospheric pressure conditions) which is rarely achieved using standard ion sources without the aid of ion compression and trapping strategies.³² To determine the "imperfections" in the tube, the experimental resolving power is often

compared to the "ideal" resolving power, or the resolving power where the full width at half maximum is a function of the gate pulse width and ideal diffusion according to Brownian motion. Such comparisons have been described by Siems et al. and Kirk et al. and will be discussed in detail below. It is worth noting that resolving power is not always classified in terms of drift time. Some reports cast resolving power in terms of ionneutral collisional cross sections, usually for non-static field instruments, which can result in mathematically inflated R_p values compared to those calculated with drift times simply due to the increased numerical values of the abscissa. Thus, all resolving powers are not directly comparable to classify instrument performance.

In this brief study, we characterize the performance of three DTIMS instruments constructed in our lab. This exercise is not only to fully characterize the existing PCBIMS design routinely used by our group, 24,38-40 but to determine whether the current PCBIMS design offers the optimum performance out of a limited selection of alternative DIY drift tube designs, and most importantly, to provide insights to the community with respect to IMS design and implementation. Each tube is based on open-source designs requiring relatively little time to assemble and made from comparatively, low-cost materials.²⁴ Designs for the respective systems are available via our group data processing and design repository (https://github.com/bhclowers/OS-IMS). The performance of each drift tube is tested using a matrix of IMS standards with a wide range of mobility values by varying the voltage and gate pulse widths within a reasonable range of operation for these instruments. Changing these two experimental variables allows us to characterize the resolving power, ideality of performance of the tube, resolution between peaks, and accuracy of recorded mobility values. The ideality of the tube is based on the characterization metrics detailed by Kirk et al., and directly compares the resolving powers experimentally determined with the theoretical resolving powers at optimized operating conditions.²⁷ Additionally, careful examination of gas-phase ion mobility provides a link to assess the accuracy and precision of the tube's performance when compared with literature values. Although separation factors are a fourth valuable metric of IMS performance, these will not be discussed in this effort. By characterizing the performance of these open-source, easy to do-it-yourself (DIY) IMS designs and

distributing a Python script for analysis, we provide a set of metrics that will allow researchers to identify an IMS design and implementation for their specific needs. Lastly, while the results presented here are for standalone, signal-averaged, DTIMS systems with a Faraday plate detector, these IMS configurations can easily be coupled to mass spectrometers.

Experimental:

Sample preparation:

A solution of 25 μM containing each of the tetraalkylammonium salts (TXA) was prepared in methanol (HPLC grade, Fisher Chemical, Fair Lawn, NJ) as described previously.⁴¹ Each of the TXA salts used were purchased from Sigma Aldrich (St. Louis, MO) and included: tetrapropyl ammonium bromide (Sigma: 225568-100G) (T3A), tetrabutyl ammonium bromide (Sigma: 426288-25G) (T4A), tetrapentyl ammonium bromide (Sigma: 241970-25G) (T5A), tetrahexyl ammonium bromide (Sigma: 252816-25G) (T6A), tetraheptyl ammonium bromide (Sigma: 87301-10G) (T7A), tetraoctyl ammonium bromide (Sigma: 294136-5G) (T8A), tetrakis-decyl ammonium bromide (Sigma: 87580-10G) (T10A), and tetradodecyl ammonium bromide (Sigma: 87249-5G) (T12A).

Instrumentation

The outlined experiments use single-gate, signal-averaged IMS instruments with drift regions and desolvation regions of varying lengths (See Figure 1). Tubes A and C were constructed as previously designed by Reinecke and Clowers.²⁴ However, Tube A's drift region used electrodes that were thinner and smaller in diameter than those previously used (Table 1).²⁴ Both of these drift cell designs follow the guidance outlined by Bohnhorst et al. to balance the inner diameter of the electrodes with electrode thickness and pitch.¹⁸ In a marked deviation from the stacked ring design, the drift region of Tube B was made of a rolled sheet of a flexible polyimide sheet with gold-coated copper electrodes (FlexIMS). Though the absolute inner diameter of the Tube B differs slightly from the report by Smith et al. ¹⁷ the design includes a "dogleg" electrode to minimize field penetration and stray fields within the drift cell (See Figure S2 and S3). One key difference in our implementation of the FlexIMS design is that the resistors are attached to a

companion FR-4 board which allows different resistor values to be rapidly exchanged. The design files for the new PCB-IMS configurations shown in this effort are included as part of the Supplementary Information and can also be found in the public repository associated with this research project (https://github.com/bhclowers/OS-IMS).

Table 1: Dimensions of the electrodes for each type of tube: mini-PCBIMS, FlexIMS, and standard PCBIMS. The electrodes for each tube are Illustrated in Figures S1-S3. It is worthy to note that different widths of the PCBIMS electrodes vary with the batch and may have a tolerance of thickness up to 0.2 mm.

	mini-PCBIMS (Tube A)	FlexIMS (Tube B)	Standard PCBIMS (Tube C)
Width of Electrode (mm)	1.0 mm	2.5 mm	1.6 mm
Inner Diameter of Electrode (mm)	14.3 mm	27.3 mm	25.0 mm
Pitch of Electrodes (mm) 2.2 mm		2.7 mm	3.8 mm

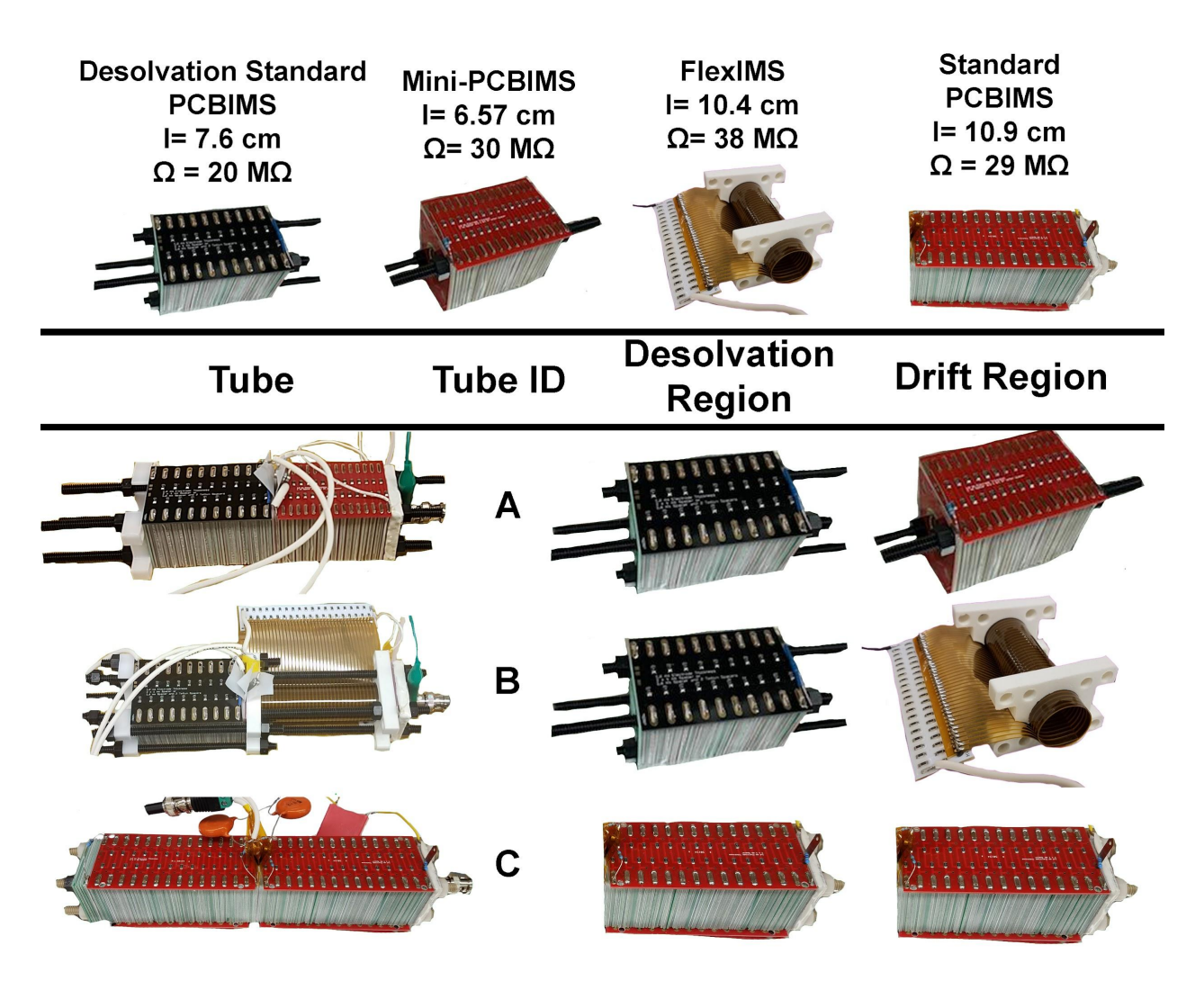


Figure 1: Visual outline of the 3 IMS tubes characterized in this set of experiments. Tube A is the mini-PCBIMS where the desolvation region is constructed of the standard diameter electrodes and spacing (with a total length of 7.6 cm), but the drift region, with a total length of 6.57 cm, is constructed with the smaller diameter electrodes with closer spacing. Tube B is the FlexIMS with the same desolvation region as Tube B, but the drift region is made of the flexible PCB design by Smith et al. with a length of 10.4 cm and a total resistance of 38 M Ω .¹⁷ Tube C is the standard design PCBIMS described previously.⁴¹

For all experiments, a countercurrent flow rate of N_2 at 0.22 L/min was added through the Faraday plate as described by Reinecke and Clowers.²⁴ Ions were generated using a custom ESI source with samples infused at a flow rate of 4 μ L/min. All of the DTIMS systems used a Faraday plate attached to a transimpedance amplifier using the design detailed by Reinecke and Clowers,²⁴ contained a tri-grid ion gate using the design as

described by Langejuergen et al., 42 and the pulse was controlled with the FET pulsers as described by Garcia et al.43 The modulation of the isolated, FET pulsers was achieved using the analog output feature of the Digilent Analog Discovery 2 (Digilent Pullman, WA) which was also synchronized with the data acquisition feature of the same USB oscilloscope. For each drift tube, a series of 36 measurements were taken containing over 1000 signals averaged spectra per measurement: six different gate pulse widths and six different electric fields as described in Table 2. The smallest gate pulse width and electric field strength were chosen from the smallest value that gives a statistically significant Gaussian peak of the lowest mobility species (T12A). The highest gate pulse width was chosen based on peak shape (i.e. when peaks are no longer Gaussian and instead, trapezoid) and the highest voltage was chosen due to concerns about dielectric breakdown. Gate pulse widths vary between tubes due to different waveform generation frequencies, each chosen based on ion drift time and to minimize spectral noise (Tube A= 41.33 Hz, Tube B= 20.33 Hz, Tube C= 23.16 Hz). The order in which the gate pulse widths were measured was randomized for each voltage. The set of six voltages, which was corrected to account for the resistance of the drift tube as described by Hauck et al., were kept constant for all 3 tubes, but due to the difference in drift tube length, results in different electric fields for each tube. 44 Each signal-averaged measurement was taken at room temperature (24-25.6 °C) and atmospheric pressures varying between 689 and 695 Torr both measured using an Omega OM-CP-PRHTEMP2000 (Omega Engineering Inc., Newark CT), with all measurements for one tube performed in a single day. Specific experimental details for each experiment are in the Supplemental Information.

Table 2: The experimental electric field settings and gate pulse widths for each drift tube

Gate Pulse Widths (µsec)			Electric Fields (V/cm)			
Tube A	Tube B	Tube C	Tube A	Tube B	Tube C	
121	98	108	441.9	479.8	438.2	
194	148	151	489.3	502.3	464.9	
242	246	259	537.7	521.7	480.8	
363	344	345	576.9	544.2	505.3	
484	492	432	622.2	563.9	532.1	
726	639	648	652.5	593.0	549.8	

Theory

While it is commonplace to characterize IMS performance by reporting resolving power, the metric itself of resolving power is often used somewhat ambiguously in the literature. The term resolution is often used when resolving power is meant, and others often define resolving power in terms of CCS measurements instead of in the time domain. As stated previously, resolving power is defined as the drift time over the full-width half maximum of the peak, as below in Equation 1:

$$R_p = \frac{t_d}{FWHM} \tag{1}$$

Despite its limitations resolving power serves as a comparison metric across different IMS platforms. Consequently, there is motivation to identify a theoretical model that will correctly predict resolving power. Siems et al. proposed such a model in 1994 based upon varying the gate pulse width, voltage, and temperature of the drift tube.²⁵ This model assumes that the full-width half max of the peak originates from 3 places: the ion gate pulse width, thermal diffusion, and any contributions to an ion's drift time such as the time spent traversing the ion optics of a mass spectrometer prior to detection. In the ideal form, there are no effects from outside the drift tube, and diffusion is predicted by the charge of the ion (z), the charge on an electron (e=1.602176 x 10⁻¹⁹ C), and the Boltzmann constant

 $(k_b=1.3806488 \ x \ 10^{-23} \ kg \ m^2 \ s^{-2} \ K^{-1})$. These variables combined with gate pulse width (t_g) , temperature (T), voltage (V), and drift time (t_d) determine the ideal full-width half-maximum in Equation 2:

$$FWHM^2 = t_g^2 + \frac{k_b * 16(\ln 2)}{ze} \frac{Tt_d^2}{V}$$
 (2)

As is the case for most models, the ideal case is rarely achieved. Instead, Siems et al. propose finding variables (gate pulse width, diffusion, and factors outside the drift tube) that describe the contributions to the full-width half-maximum empirically.²⁵ Empirically, these relationships transform into Equation 3:

$$FWHM^2 = \gamma + \beta t_g^2 + \alpha \frac{Tt_d^2}{V}$$
 (3)

Where α is the diffusion term, β is the gate pulse width term, and γ is the time spent outside of the drift tube. If the ideal form was obeyed, then each of the variables would respectively be, β = 1, γ =0 (ms²), and α = 0.957 x 10⁻³ Volts/ Kelvin. However, this method requires knowledge of multiple experimental parameters across the suite of experimental measurements that include varying temperature, voltage, and gate pulse width for each tube (which may not be practical for all drift tube configurations).

Another notable effort to classify drift tube performance came from Kirk et al., where they inserted the derivative of Equation 2 with respect to voltage into Equation 1 to obtain the optimum voltage (V_{opt}) that would give the optimum resolving power of the drift tube.²⁷ The result is Equation 4 below:

$$V_{opt} = \sqrt[3]{\frac{8k_b T (ln2)L^4}{zeK_0^2 t_g^2}} \tag{4}$$

The variables and constants are the same as those in Equation 2 with the addition of the drift tube's length (L) and the reduced mobility (K_0). Through a few assumptions, Equation

4 can be inserted into Equation 1 and the ideal resolving power ratio to measure drift tube performance in Equation 5 is obtained:

$$Ideality = \frac{1}{26.4} \sqrt{\frac{R_{max,meas}^2}{V_{max,meas}}}$$
 (5)

Where R_{max,meas} is the maximum resolving power captured within the range of voltages tested, V_{max,meas} is the voltage at which R_{max,meas} was measured, and T is the temperature. The ideality given here is a ratio of the drift tube's performance over the "ideal" case and will be 1 where the drift tube performance is ideal. Equation 5 also assumes the charge state of the ion is 1 and instead the 1/26.4 term is changed if the charge is higher than 1.²⁷ However, Equation 5 also assumes the optimum resolving power for the tube is the maximum resolving power measured when varying the electric field strength during an instrumental characterization experiment.

As a brief note, resolution as degree of separation between two peaks is defined below in Equation 6:

$$R = \frac{2(t_{d1} - t_{d2})}{(w_1 + w_2)} \tag{6}$$

Where t_{d1} is the drift time of Ion 1, t_{d2} is the drift time of Ion 2, w_1 and w_2 are the full peak widths of ions 1 and 2 respectively. R is the resolution, where partial separation of peaks occurs when R=1 and peaks are considered fully separated if R = 1.5.

Results/ Discussion

Resolving Powers

Table 3: The range of experimental resolving powers measured for the analytes for each tube. The average resolving power (and one standard deviation) reported is for all voltages measured at one gate pulse width per tube as follows: Tube A= 194 μ sec, Tube B= 148 μ sec, Tube C= 151 μ sec.

	mini-PCBIMS (Tube A)		FlexIMS (Tube B)			Standard PCBIMS (Tube C)			
	Min R _p	Max R _p	Average R _p	Min R _p	Max R _p	Average R _p	Min R _p	Max R _p	Average R _p
ТЗА	10.4	48.2	38 ± 8	16.1	61.9	49 ± 5	20.0	91.8	83 ± 7
T4A	12.7	61.2	50 ± 5	19.0	65.8	54 ± 4	23.2	107	82 ± 8
T5A	14.6	63.0	54 ± 5	21.7	69.2	58 ± 4	26.6	103	96 ± 4
T6A	16.3	67.9	60 ± 5	24.0	69.8	62 ± 4	29.7	107	97 ± 3
T7A	18.9	69.7	58 ± 9	27.3	72.4	64 ± 5	33.4	105	94 ± 8
T8A	20.3	70.9	62 ± 7	29.4	74.6	65 ± 3	36.7	106	99 ±5
T10A	21.8	73.4	65 ± 6	31.6	70.0	64 ± 2	41.9	89	74 ± 10
T12A	24.7	77.9	63 ± 11	36.7	70.8	65 ± 5	45.9	108	81 ±15

Evaluating the maximum, minimum, and average resolving powers in Table 3 and Figure 2 highlights specific trends across the different drift tube constructions and explicitly includes the impact of gate pulse width and electric field strength. The mini-PCBIMS and FlexIMS have comparable maximum and average resolving powers in Table 3. While the average and range resolving powers in Table 3 are the same within a standard deviation, the second smallest gate pulse widths themselves differ by 50 µsec. Additionally, the FlexIMS and standard PCBIMS have comparable minimum resolving powers which are likely due to the similar length of both tubes. The maximum resolving powers for the FlexIMS is marginally lower than the obtained maximum resolving powers of 80 by both Smith et al. and Chantipmannee and Hauser. 17,45 The maximum and average resolving

power for the standard PCBIMS is significantly the highest of all the tubes and is comparable to what has been previously reported using this IMS design with signal-averaged mode.^{38,39} However, a closer examination of Figure 2 shows that the FlexIMS and the standard PCBIMS also have the most consistent resolving powers as a function of the gate pulse widths. For all tubes, the shortest gate pulse widths have the highest overall resolving powers (when there are enough ions present to generate a statistically significant peak for peak fitting); however, the highest resolving powers do not necessarily translate to the highest ideality (Figure 3).

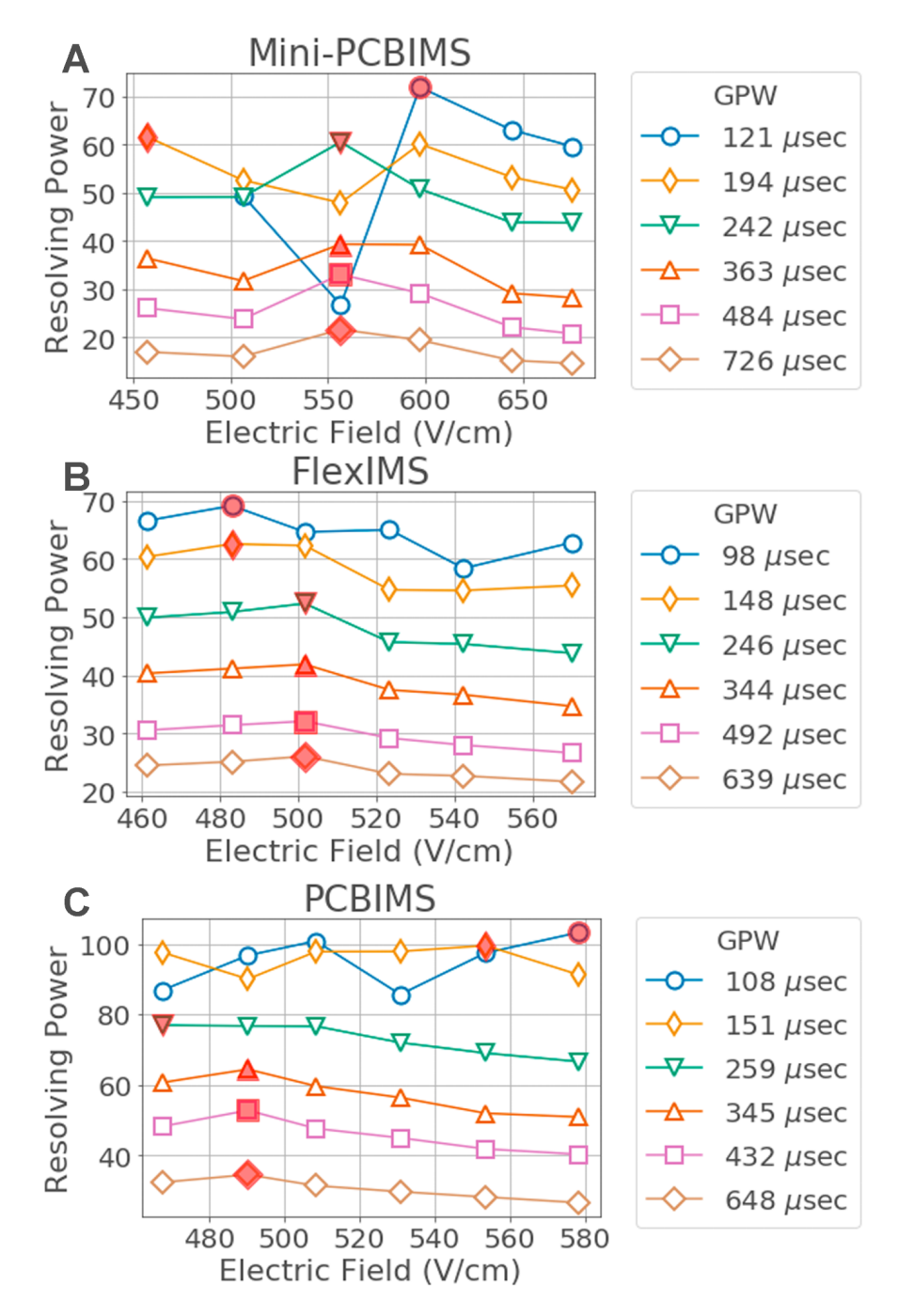


Figure 2: Examining the plots of resolving power for T5A against the applied electric field for each drift tube, both the maximum and minimum resolving powers are shown as each trace is a different gate pulse width. To find the ideal resolving power ratio described by Kirk et al., the maximum resolving power for each gate pulse width used to calculate the ideal R_p is marked with a filled red marker.²⁷

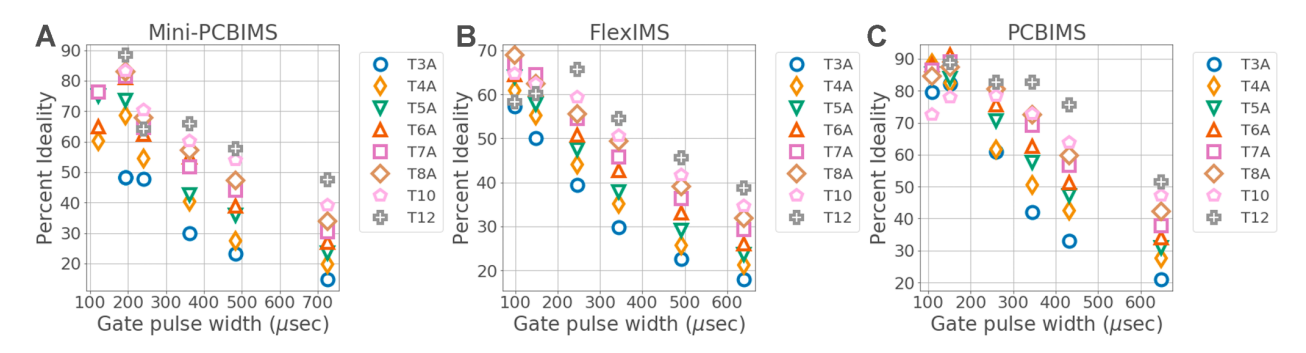


Figure 3: The ideality of the drift tube graphs calculated using the method described by Kirk et al. are presented here.²⁷ The PCBIMS, both standard and mini, show similar trends and ranges of ideality; both reach a peak of close to 90% ideality at 150 μsec before declining as the gate pulse width increases. The FlexIMS reaches an ideality maximum of only 70% before declining. All tubes reach the lowest ideality ratio (between 20-50% depending on analyte) at the largest gate pulse widths.

Using the maximum resolving powers from all species (such as T5A shown in Figure 2) and inserting those values into Equation 5 yields the data shown in Figure 3. For all drift tubes, the highest "ideality" is accordingly at the lowest gate pulse widths. The lowest "ideality" is at the largest gate pulse width and spans a similar range for all tubes (20-50%) ideality depending on ion identity). However, there are two notable differences when comparing the tubes: the range of ideality the ions occupy per gate pulse width and the maximum percent ideality for each tube. For multiple ions in the mini-PCBIMS and PCBIMS designs, the maximum ideality is reached at the second smallest gate pulse widths, 194 µsec and 148 µsec, respectively. Because maximum ideality is not at the smallest gate pulse width, the gates are likely not operating as effectively as expected. The previously reported tri-state shutter gating scheme could be one possible solution to minimize gate depletion in the present designs and improve the ideality ratio and is a future topic worth examining. 38,46 Additionally, with the PCB designs (both mini and standard), the maximum ideality is higher than the rest of the designs, reaching a maximum of >90% in both tubes. The standard PCBIMS design also boasts the highest resolving powers (Table 3) and the smallest range of ideality per analyte at lower gate pulse widths (12% difference in ideality).

However, the FlexIMS offers the most predictable levels of ideality where a linear fit could be applied to each analyte as a function of the gate pulse width. It is worth noting that the ideality of the flexible IMS from Chantipmanee and Hauser is 83% at a 200 μ sec gate pulse width, higher than our results at even the lowest gate pulse widths we tested. Their higher ideality is likely due to the higher resolving powers they achieved, but another very plausible explanation is due to the difference between their flexible drift tube design and ours. They modeled the pitch and width of the electrodes of their flexible drift tube after the standard PCBIMS design of Reinecke and Clowers presented here, and when comparing their flexible drift tube and our standard PCBIMS, both the range of resolving powers (R_p = 79 for T5A for 259 μ sec in Figure 2) and the ideality of the tube (between 75-85% ideality for 200 μ sec based on Figure 3) agree with each other. The similarities between these tubes indicates that the different pitch and width of the electrodes in our FlexIMS may explain why the performance differs compared to similar efforts in the literature (Table 1) and deserves a more thorough examination in the future.

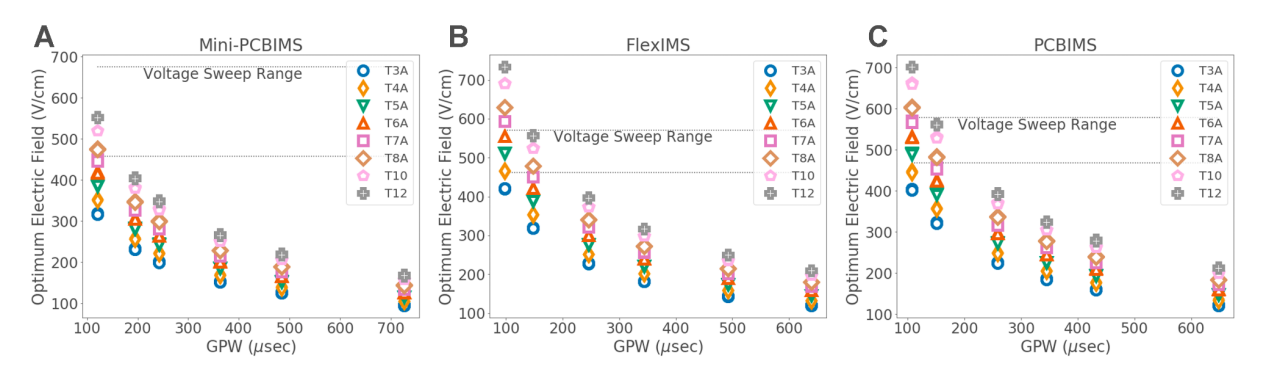


Figure 4: Using the equation found by Kirk et al. in Equation 4, the optimum voltage for each gate pulse width was calculated.²⁷ In addition, the range of voltages used in this set of experiments is within dotted lines shown. For the FlexIMS, PCBIMS, and mini-PCBIMS, the optimum voltage of only a few of the ions is within the voltage range used in the experiment.

At medium to large gate pulse widths, all analytes for all tubes showed the same range of ideality. Specifically, for a single analyte, the ideality differs by less than 20% both for a single tube once gate pulse widths are larger than 300 µsec, and between tubes for the same analyte and gate pulse width. The broad distribution of idealities across all gate pulse widths could be due to gating inefficiencies, but another more likely explanation is shown in Figure 4. Figure 4 illustrates the optimum voltage that will give the maximum

resolving power for the tube (conditions under which it was tested) as calculated by Equation 4 graphed as a function of the gate pulse width. The actual range of electric fields tested in Table 1 is imposed as dotted lines marking the range of experimentally tested fields. Equation 5 assumes the maximum resolving power measured within the experiment *is* the maximum resolving power at the optimum voltage in Equation 4. If the measured maximum resolving power occurs at a different voltage than the result from Equation 4, the function that governs the ideal resolving power will be different from the actual function for the maximum resolving power.

It is worthy to note that for the mini-PCBIMS, the FlexIMS, and the standard PCBIMS, a few analytes fall within the range for the optimum voltage for one or two gate pulse widths. For these analytes, the ideal resolving power is 65-70% for both the mini-PCBIMS and FlexIMS but is 75-85% for the standard PCBIMS. These should be considered the "percent idealities" for these tubes since these maximum voltages fall within the range of the voltages tested. While the percent idealities are reasonable, it is worth noting possible inhomogeneous electric field effects around the ion gate may explain reduced performance than expected for the FlexIMS. Preliminary results show that when a few extra PCBIMS electrodes are placed between the gate and FlexIMS, resolving power is increased, which more closely approaches theory (Figure S10). The electric fields around the gates for the FlexIMS may also be optimized by adding a variable resistor between the last electrode on the kapton sheet and the gate itself to allow for fine-tuning the field around the gate. This approach may result in a further increase in resolving power that more closely approaches theory but requires further investigation.

However, caution is warranted when judging a drift tube solely by how closely the resolving power matches the theoretical maximum in the ideality ratio for a few reasons. Most reasons arise from practical limitations. The maximum resolving power occurs at smaller gate pulse widths over a range of voltages depending on analyte (Figure 4). For ions with slower drift times the ion likely will not be detectable at the gate under these optimized experimental conditions due to combined factors of gate depletion effect and prolonged diffusion from longer drift times. For ions with faster drift times, the optimum

voltage may not be physically achievable due to dielectric breakdown concerns or the maximum voltage output from the available power supplies. Additionally, as illustrated in Figure 4, a wide range of electric field strengths would be needed to optimize every peak in a complex sample matrix at single gate pulse width. This is impractical for complex sample matrices or in cases where an analyte may have multiple peaks, e.g. proteins and other biologically relevant molecules. Finally, optimizing the voltage requires knowing of the mobility of the analyte before the experiment is conducted, which is a scenario that is not always true. While the ideality ratio in Equation 5 can be useful to guide a selection of experimental parameters, it should not be the only metric considered in choosing the best-suited DIY-IMS design.

Resolution

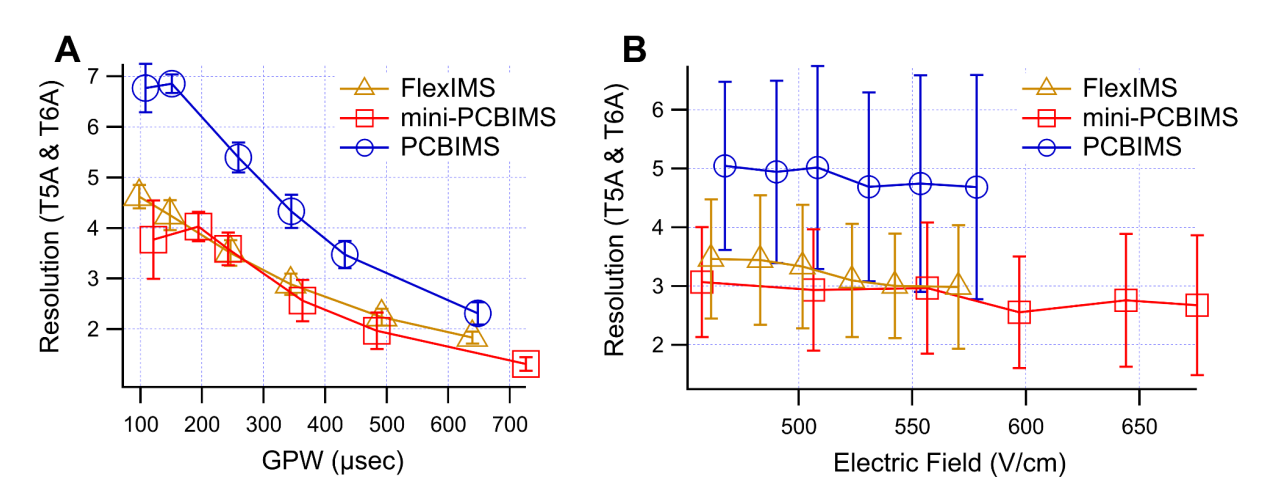


Figure 5: The resolution (separation of two peaks) between T5A and T6A as a function of gate pulse width **(A)** and electric field strength **(B)** are shown for all three tubes tested here. For all tubes, the highest resolution is at the lowest gate pulse widths. Resolution is largely constant as a function of electric field strength showing, in this case, separation between peaks is most dependent on gate pulse width. All peaks across all settings are baseline separated.

Worthy of a quick note is the resolution (Equation 6) of all three tubes since resolution is closely related to revolving power. Figure 5 shows the resolution of all measurements of all tubes as a function of gate pulse width and electric field strength. Since the

measurements here were performed in a matrix and difficult to visualize, all electric field strengths (average and one standard deviation) are plotted for each gate pulse width in Figure 5A, and vice versa for gate pulse width and electric field in Figure 5B. T5A and T6A were chosen to compare resolution (separation of two peaks) since these two peaks have some of the highest peak intensities across all experimental settings and drift times relatively in the middle of the range of salts tested. Unsurprisingly, lower gate pulse widths increase resolution due to narrower peak widths. Resolution is unchanged by electric field strength within error because the averages in Figure 5B are the same and error is small in Figure 5A. Out of the drift tubes, the results are similar to the average resolving powers listed in Table 3. The standard PCBIMS has the highest average resolution (and highest average resolving powers) whereas the FlexIMS and mini-PCBIMS have the same resolutions as a function of gate pulse width and voltage within error. While resolving power is related to resolution, one metric may be of more value to experimentalists than the other based upon application.

Measurement of Reduced Mobilities

The last point of discussion for the comparison of these tubes is whether they can give accurate and precise reduced mobilities. Determination of accurate mobility values is an important metric of performance with regards to identifying unknown analytes, for instance identification of compounds relevant for security applications. ^{11,44} Without accurate K₀ values, unknown compounds cannot be correctly identified, despite how high the resolving power of the instrument might be. Furthermore, all tubes presented here are capable of measuring first-principles reduced mobility values. The exact length of the tubes is known (depending on accuracy of calipers), and ambient temperature and pressures are measured with a NIST-traceable atmospheric gauge. Therefore, the accuracy of mobility values from each of these tubes is dependent on the accuracy of the variables present in the reduced mobility equation. Stated differently, these tubes are not dependent on calibration techniques.

Worthy of note here is that since all these tubes are ambient temperature, the desolvation region's length directly impacts the reduced mobilities. Shorter desolvation regions may result in smaller K₀ values due to ions not being fully desolvated. No significant impact on the mobilities are observed due to the difference of 3.3 cm in the desolvation region length between Tubes A and B, and Tube C and the reference Naylor et al.³⁹ However, TXA salts have been suggested as an appropriate IMS standard because of their low water binding affinity (i.e. they don't like to cluster). While we did not observe differences in mobility related to clustering for all desolvation region lengths, the results may vary if other compounds with higher water binding energies are used when accessing appropriate desolvation region length.

For all of the tubes in Table 4, the K₀ values are within error of each other indicating that all tubes tested here give accurate values, despite minor differences in the average values. The K₀ values are directly calculated using the parameters measured during the experiment (drift time, tube length, voltage, pressure, and temperature) and are not obtained from calibration; the average and error (one standard deviation) are obtained from all 36 GPW and voltage measurements performed on the tubes. Two additional clarifications are needed to bound the expectations of assessment of accuracy of these K₀ values, however. First, Table 4 contains mobility values previously published from our group on a completely different instrument (PCBIMS-TIMS-TOF) as the literature mobility values.³⁹ We are not saying we have the definitive "correct" K₀ values for TXA salts, just that these values are used as the comparison for the results presented in this effort. Second, to our knowledge, there is no NIST-tracable IMS calibrant standard that can be used to fully assess IMS accuracy. With regards to precession, interestingly, the FlexIMS has the lowest error associated with the K₀ values for all analytes suggesting that the shielding effect of the dogleg in the electrode design provides more consistent performance in drift times which results in more consistent mobilities.

Table 4: The average reduced mobility values of the analytes (cm² V⁻¹ sec⁻¹) and length of the desolvation regions for each tube.

	mini- PCBIMS (Tube A)	FlexIMS (Tube B)	Standard PCBIMS (Tube C)	Naylor et al. ³⁹
T3A	1.44 ± 0.02	1.440 ± 0.006	1.43 ± 0.01	1.444 ± 0.008
T4A	1.23 ± 0.02	1.237 ± 0.004	1.228 ± 0.009	1.236 ± 0.008
T5A	1.072 ± 0.009	1.074 ± 0.002	1.065 ± 0.007	1.073 ± 0.007
T6A	0.950 ± 0.006	0.951 ± 0.001	0.943 ± 0.006	0.948 ± 0.007
T7A	0.857 ± 0.006	0.859 ± 0.002	0.850 ± 0.004	0.855 ± 0.005
T8A	0.784 ± 0.005	0.786 ± 0.001	0.778 ± 0.004	0.782 ± 0.005
T10A	0.682 ± 0.004	0.685 ± 0.001	0.678 ± 0.003	0.681 ± 0.005
T12A	0.624 ± 0.003	0.6257 ± 0.0009	0.619 ± 0.002	0.620 ± 0.004
Desolv. Region Length	7.6 cm	7.6 cm	10.9 cm	10.9 cm

Conclusion

Presented here are the results of comparing three distinctive drift tube designs evaluating them in terms of accurate/precise mobility values, resolution, and resolving powers. All drift tubes produced accurate mobilities for each analyte within a standard deviation compared to literature. The FlexIMS K_0 values had the least error associated with them, likely due to the field focusing effect of the dogleg electrode design. As for resolving powers, the standard PCBIMS had the highest resolving powers ($R_p > 90$ at best for most analytes) and the highest resolution compared to the other IMS designs. Additionally, the ideality of each drift tube is evaluated according to the method proposed by Kirk et al.²⁷ By this metric for the analytes where the electric field sweep covered the optimum calculated voltage from Equation 4, the PCBIMS performed the best with 75-85% ideally compared to the 60-70% ideality of the mini-PCBIMS and FlexIMS. Depending on the

desired application of the IMS in question, the FlexIMS gives the most precise K₀ values,

whereas the PCBIMS gives the highest resolving power and resolution. The resolving

power of these tubes can be further improved by implementing the tri-state shutter gating

scheme as detailed by Kirk et al. but was not explored in this work.⁴⁶ Additionally, all tubes

have higher resolving powers, even at unoptimized conditions, than most commercial drift

tube instruments (with a max reported resolving power of less than 70) and give accurate

and precise mobilities of the analytes tested. 13,47 The drift tubes' performance presented

here, therefore, offers a low-cost alternative for other forms of IMS instrumentation that

provide comparable performance to commercial options.

Associated Content:

Supplementary Material:

The supporting document further detailing drift tube construction and results from

the hybrid IMS design are included in the associated file. An example data set and the

associated processing script can be found in the Supplementary Information. Additional

data sets associated with this manuscript are available upon request. Designs for the

associated electronics and *IMS* electrodes can be found at

https://github.com/bhclowers/OS-IMS.

Author Information:

Corresponding author: *Brian Clowers; brian.clowers@wsu.edu

ORCID:

Cameron N. Naylor: 0000-0002-3426-0367

Elvin R. Cabrera: 0000-0003-3342-0231

Brian H. Clowers: 0000-0002-5809-9379

Author Declarations

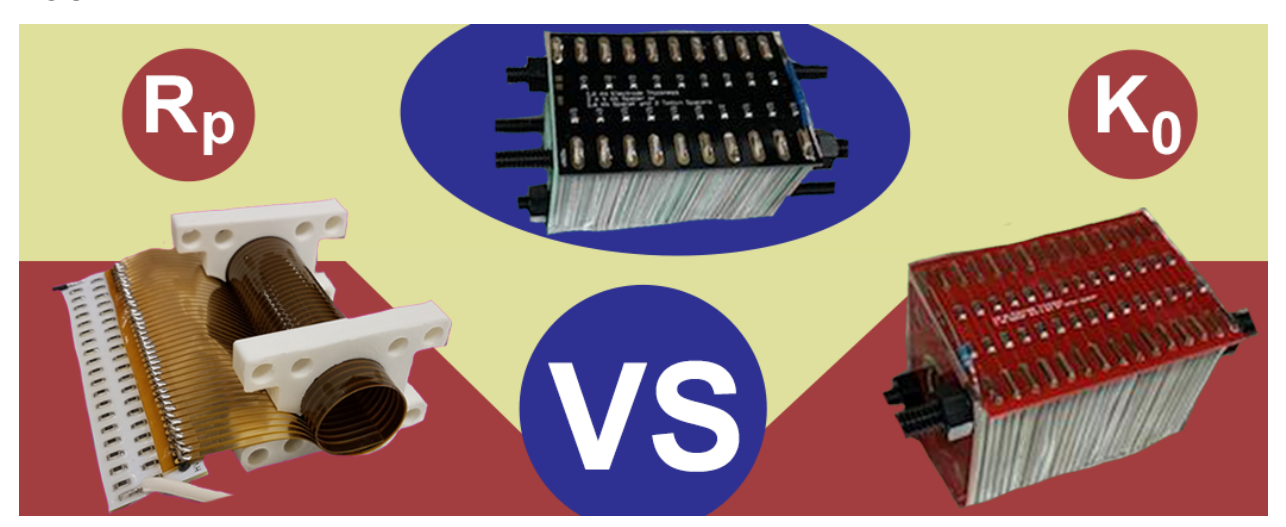
The authors have no conflicts to disclose.

22

Acknowledgments:

Support for CNN and ERC was provided by NSF-CHE 2003042 and NIH R01GM138863, respectively. We also want to thank Dr.-Ing Ansgar T. Kirk for helpful comments in clarifying some of the points reported in Reference 27.

TOC



Three low-cost drift tube ion mobility spectrometers are analyzed for resolving power, resolution, and accuracy of reduced mobilities.

References

- (1) Bush, M. F.; Hall, Z.; Giles, K.; Hoyes, J.; Robinson, C. V.; Ruotolo, B. T. Collision Cross Sections of Proteins and Their Complexes: A Calibration Framework and Database for Gas-Phase Structural Biology. *Anal. Chem.* **2010**, *82* (22), 9557–9565.
- (2) Pierson, N. A.; Valentine, S. J.; Clemmer, D. E. Evidence for a Quasi-Equilibrium Distribution of States for Bradykinin [M + 3H]3+ Ions in the Gas Phase. *J. Phys. Chem. B* **2010**, *114* (23), 7777–7783.
- (3) Shi, H.; Pierson, N. A.; Valentine, S. J.; Clemmer, D. E. Conformation Types of Ubiquitin [M+8H]8+ Ions from Water:methanol Solutions: Evidence for the N and A States in Aqueous Solution. *J. Phys. Chem. B* **2012**, *116* (10), 3344–3352.
- (4) May, J. C.; McLean, J. A. Ion Mobility-Mass Spectrometry: Time-Dispersive Instrumentation. *Anal. Chem.* **2015**, *87* (3), 1422–1436.
- (5) May, J. C.; Morris, C. B.; McLean, J. A. Ion Mobility Collision Cross Section Compendium. *Anal. Chem.* **2017**, 89 (2), 1032–1044.
- (6) Hernandez, D. R.; DeBord, J. D.; Ridgeway, M. E.; Kaplan, D. A.; Park, M. A.; Fernandez-Lima, F. Ion Dynamics in a Trapped Ion Mobility Spectrometer. *Analyst* **2014**, *139* (8), 1913–1921.
- (7) Silveira, J. A.; Ridgeway, M. E.; Park, M. A. High Resolution Trapped Ion Mobility Spectrometery of Peptides. *Anal. Chem.* **2014**, *86* (12), 5624–5627.
- (8) Giles, K.; Pringle, S. D.; Worthington, K. R.; Little, D.; Wildgoose, J. L.; Bateman, R. H. Applications of a Travelling Wave-Based Radio-Frequency-Only Stacked Ring Ion Guide. *Rapid Commun. Mass Spectrom.* **2004**, *18* (20), 2401–2414.
- (9) Pringle, S. D.; Giles, K.; Wildgoose, J. L.; Williams, J. P.; Slade, S. E.; Thalassinos, K.; Bateman, R. H.; Bowers, M. T.; Scrivens, J. H. An Investigation of the Mobility Separation of Some Peptide and Protein Ions Using a New Hybrid Quadrupole/travelling Wave IMS/oa-ToF Instrument. *Int. J. Mass Spectrom.* **2007**, *261* (1), 1–12.
- (10) Webb, I. K.; Garimella, S. V. B.; Tolmachev, A. V.; Chen, T.-C.; Zhang, X.; Norheim, R. V.; Prost, S. A.; LaMarche, B.; Anderson, G. A.; Ibrahim, Y. M.; Smith, R. D. Experimental Evaluation and Optimization of Structures for Lossless Ion Manipulations for Ion Mobility Spectrometry with Time-of-Flight Mass Spectrometry. *Anal. Chem.* **2014**, *86* (18), 9169–9176.
- (11) Ewing, R. G.; Atkinson, D. A.; Eiceman, G. A.; Ewing, G. J. A Critical Review of Ion Mobility Spectrometry for the Detection of Explosives and Explosive Related Compounds. *Talanta* **2001**, *54* (3), 515–529.
- (12) Mäkinen, M. A.; Anttalainen, O. A.; Sillanpää, M. E. T. Ion Mobility Spectrometry and Its Applications in Detection of Chemical Warfare Agents. *Anal. Chem.* **2010**, *82* (23), 9594–9600.
- (13) May, J. C.; Dodds, J. N.; Kurulugama, R. T.; Stafford, G. C.; Fjeldsted, J. C.; McLean, J. a. Broadscale Resolving Power Performance of a High Precision Uniform Field Ion Mobility-Mass Spectrometer. *Analyst* **2015**, *140* (20), 6824–6833.
- (14) Kurulugama, R. T.; Darland, E.; Kuhlmann, F.; Stafford, G.; Fjeldsted, J. Evaluation of Drift Gas Selection in Complex Sample Analyses Using a High Performance Drift Tube Ion Mobility-QTOF Mass Spectrometer. *Analyst* **2015**, *140* (20), 6834–6844.
- (15) Morrison, K. A.; Siems, W. F.; Clowers, B. H. Augmenting Ion Trap Mass Spectrometers Using a Frequency Modulated Drift Tube Ion Mobility Spectrometer. *Anal. Chem.* **2016**, *88* (6), 3121–3129.
- (16) Kwantwi-Barima, P.; Ouyang, H.; Hogan, C. J., Jr; Clowers, B. H. Tuning Mobility Separation Factors of Chemical Warfare Agent Degradation Products via Selective Ion-

- Neutral Clustering. Anal. Chem. 2017, 89 (22), 12416–12424.
- (17) Smith, B. L.; Boisdon, C.; Young, I. S.; Praneenararat, T.; Vilaivan, T.; Maher, S. Flexible Drift Tube for High Resolution Ion Mobility Spectrometry (Flex-DT-IMS). *Anal. Chem.* **2020**, 92 (13), 9104–9112.
- (18) Bohnhorst, A.; Kirk, A. T.; Zimmermann, S. Simulation Aided Design of a Low Cost Ion Mobility Spectrometer Based on Printed Circuit Boards. *Int. J. Ion Mobil. Spectrom.* **2016**, 19 (2), 167–174.
- (19) Ahrens, A.; Hitzemann, M.; Zimmermann, S. Miniaturized High-Performance Drift Tube Ion Mobility Spectrometer. *Int. J. Ion Mobil. Spectrom.* **2019**, *22* (2), 77–83.
- (20) Ahrens, A.; Möhle, J.; Hitzemann, M.; Zimmermann, S. Novel Ion Drift Tube for High-Performance Ion Mobility Spectrometers Based on a Composite Material. *Int. J. Ion Mobil. Spectrom.* **2020**, *23* (2), 75–81.
- (21) Bohnhorst, A.; Hitzemann, M.; Lippmann, M.; Kirk, A. T.; Zimmermann, S. Enhanced Resolving Power by Moving Field Ion Mobility Spectrometry. *Anal. Chem.* **2020**, *92* (19), 12967–12974.
- (22) Hauck, B. C.; Ruprecht, B. R.; Riley, P. C.; Strauch, L. D. Reproducible 3D-Printed Unibody Drift Tubes for Ion Mobility Spectrometry. *Sens. Actuators B Chem.* **2020**, 323, 128671.
- (23) Hollerbach, A.; Fedick, P. W.; Cooks, R. G. Ion Mobility-Mass Spectrometry Using a Dual-Gated 3D Printed Ion Mobility Spectrometer. *Anal. Chem.* **2018**, *90* (22), 13265–13272.
- (24) Reinecke, T.; Clowers, B. H. Implementation of a Flexible, Open-Source Platform for Ion Mobility Spectrometry. *HardwareX* **2018**, *4*. https://doi.org/10.1016/j.ohx.2018.e00030.
- (25) Siems, W. F.; Wu, C.; Tarver, E. E.; Hill, H. H. J.; Larsen, P. R.; McMinn, D. G. Measuring the Resolving Power of Ion Mobility Spectrometers. *Anal. Chem.* **1994**, *66* (23), 4195–4201.
- (26) Rokushika, S.; Hatano, H.; Baim, M. a.; Hill, H. H. Resolution Measurement for Ion Mobility Spectrometry. *Anal. Chem.* **1985**, *57* (9), 1902–1907.
- (27) Kirk, A. T.; Bakes, K.; Zimmermann, S. A Universal Relationship between Optimum Drift Voltage and Resolving Power. *Int. J. Ion Mobil. Spectrom.* **2017**, *20* (3), 105–109.
- (28) Asbury, G. R.; Hill, H. H. Using Different Drift Gases To Change Separation Factors (α) in Ion Mobility Spectrometry. *Anal. Chem.* **2000**, 72 (3), 580–584.
- (29) Beegle, L. W.; Kanik, I.; Matz, L.; Hill, H. H. Effects of Drift-Gas Polarizability on Glycine Peptides in Ion Mobility Spectrometry. *Int. J. Mass Spectrom.* **2002**, *216* (3), 257–268.
- (30) Matz, L. M.; Hill, H. H., Jr. Evaluation of Opiate Separation by High-Resolution Electrospray Ionization-Ion Mobility Spectrometry/mass Spectrometry. *Anal. Chem.* **2001**, 73 (8), 1664–1669.
- (31) Kanu, A. B.; Gribb, M. M.; Hill, H. H. J. Optimal Resolving Power for Ambient Pressure Ion Mobility Spectrometry (IMS). *Anal. Chem.* **2008**, *80* (17), 6610–6619.
- (32) Eiceman, G. A.; Nazarov, E. G.; Rodriguez, J. E.; Stone, J. A. Analysis of a Drift Tube at Ambient Pressure: Models and Precise Measurements in Ion Mobility Spectrometry. *Rev. Sci. Instrum.* **2001**, *72* (9), 3610–3621.
- (33) Benigni, P.; Porter, J.; Ridgeway, M. E.; Park, M. A.; Fernandez-Lima, F. Increasing Analytical Separation and Duty Cycle with Nonlinear Analytical Mobility Scan Functions in TIMS-FT-ICR MS. *Anal. Chem.* **2018**, *90* (4), 2446–2450.
- (34) Deng, L.; Webb, I. K.; Garimella, S. V. B.; Hamid, A. M.; Zheng, X.; Norheim, R. V.; Prost, S. A.; Anderson, G. A.; Sandoval, J. A.; Baker, E. S.; Ibrahim, Y. M.; Smith, R. D. Serpentine Ultralong Path with Extended Routing (SUPER) High Resolution Traveling Wave Ion Mobility-MS Using Structures for Lossless Ion Manipulations. *Anal. Chem.* **2017**, 89 (8), 4628–4634.
- (35) Nagy, G.; Attah, I. K.; Garimella, S. V. B.; Tang, K.; Ibrahim, Y. M.; Baker, E. S.; Smith, R. D. Unraveling the Isomeric Heterogeneity of Glycans: Ion Mobility Separations in Structures for Lossless Ion Manipulations. *Chem. Commun.* **2018**, *54* (83), 11701–11704.
- (36) Campuzano, I. D. G.; Giles, K. Historical, Current and Future Developments of Travelling

- Wave Ion Mobility Mass Spectrometry: A Personal Perspective. *Trends Analyt. Chem.* **2019**, *120*, 115620.
- (37) Adams, K. J.; Montero, D.; Aga, D.; Fernandez-Lima, F. Isomer Separation of Polybrominated Diphenyl Ether Metabolites Using nanoESI-TIMS-MS. *Int. J. Ion Mobil. Spectrom.* **2016**, *19* (2), 69–76.
- (38) Kwantwi-Barima, P.; Reinecke, T.; Clowers, B. H. Increased Ion Throughput Using Tristate Ion-Gate Multiplexing. *Analyst* **2019**, *144* (22), 6660–6670.
- (39) Naylor, C. N.; Reinecke, T.; Ridgeway, M. E.; Park, M. A.; Clowers, B. H. Validation of Calibration Parameters for Trapped Ion Mobility Spectrometry. *J. Am. Soc. Mass Spectrom.* **2019**, *30* (10), 2152–2162.
- (40) Reinecke, T.; Davis, A. L.; Clowers, B. H. Determination of Gas-Phase Ion Mobility Coefficients Using Voltage Sweep Multiplexing. *J. Am. Soc. Mass Spectrom.* **2019**, *30* (6), 977–986.
- (41) Naylor, C. N.; Reinecke, T.; Clowers, B. H. Assessing the Impact of Drift Gas Polarizability in Polyatomic Ion Mobility Experiments. *Anal. Chem.* **2020**, *92* (6), 4226–4234.
- (42) Langejuergen, J.; Allers, M.; Oermann, J.; Kirk, A.; Zimmermann, S. High Kinetic Energy Ion Mobility Spectrometer: Quantitative Analysis of Gas Mixtures with Ion Mobility Spectrometry. *Anal. Chem.* **2014**, *86* (14), 7023–7032.
- (43) Garcia, L.; Saba, C.; Manocchio, G.; Anderson, G. A.; Davis, E.; Clowers, B. H. An Open Source Ion Gate Pulser for Ion Mobility Spectrometry. *Int. J. Ion Mobil. Spectrom.* **2017**, *20* (3-4), 87–93.
- (44) Hauck, B. C.; Siems, W. F.; Harden, C. S.; McHugh, V. M.; Hill, H. H. E/N Effects on K0 Values Revealed by High Precision Measurements under Low Field Conditions. *Rev. Sci. Instrum.* **2016**, *87* (7), 075104.
- (45) Chantipmanee, N.; Hauser, P. C. Development of Simple Drift Tube Design for Ion Mobility Spectrometry Based on Flexible Printed Circuit Board Material. *Anal. Chim. Acta* **2021**, 338626.
- (46) Kirk, A. T.; Grube, D.; Kobelt, T.; Wendt, C.; Zimmermann, S. High-Resolution High Kinetic Energy Ion Mobility Spectrometer Based on a Low-Discrimination Tristate Ion Shutter. *Anal. Chem.* **2018**, *90* (9), 5603–5611.
- (47) Hilton, C. K.; Krueger, C. A.; Midey, A. J.; Osgood, M.; Wu, J.; Wu, C. Improved Analysis of Explosives Samples with Electrospray Ionization-High Resolution Ion Mobility Spectrometry (ESI-HRIMS). *Int. J. Mass Spectrom.* **2010**, 298 (1), 64–71.